Point-spread function reconstruction for the ground layer adaptive optics system ARGOS

D. Peter[a]

[a]Max-Planck-Institut für Astronomie, Koenigstuhl 17, Heidelberg, Germany

ABSTRACT

ARGOS is the ground layer adaptive optics system planned for the LBT. Although ground layer adaptive optics systems provide a relatively homogeneous point spread function over the full field of view there will be still variations of the order of a few 10%. In the case of a laser based GLAO system these variations are mostly due to the facts that only one auxiliary guide star is used and to the cone effect. Astrometry and photometry on AO corrected images are effected by these changes in the shape of the point spread function with field angle. To reduce this effect for the ARGOS system a scheme for point spread function reconstruction from wavefront sensor data is developed. The scheme uses the wavefront sensor data twofold: To reconstruct the wavefront and to measure the atmospheric profile via SLODAR. The reconstruction scheme is tested in simulations of the full system for various seeing conditions and guide star angles. The quality of the reconstruction is tested in simulation.

Keywords: Adaptive optics, ground layer AO, Point spread function, PSF reconsruction, wide field

1. THE ARGOS SYSTEM

ARGOS[1] is the ground layer adaptive optics (GLAO) system for the LBT. The system recently passed the FDR and will be at the telescope at mid 2012. It is designed to act as seeing reducer for the LUCIFER instrument.[2]The goal is to reduce the full width at half maximum (FWHM) on the science image by a factor of two for a wide range of atmospheric conditions. This will improve the spatial resolution on the image and save observing time. A schematic image of ARGOS is shown in Figure 1.

In the following I will describe the details of the system relevant for this paper. The discussion will take place on a single eye of the telescope as there is no interaction foreseen between both eyes of the telescope.

For measurement of high order modes ARGOS will use three lasers which are positioned on a circle with 2' radius at a height of 12 km. The lasers will be equally spaced, i.e., with an angle of 120° on the circle between them. The tip and tilt (TT-)modes will be measured by a TT-wavefront sensor (WFS) using a natural guide star. This star can be anywhere in the FOV of LUCIFER which is 4' x 4'. The measurement is done by three 15x15 Shack Hartmann wavefront sensor (SWS) for the lasers and a quad cell detector for the TT-modes. The entire reconstructed wavefront is applied to the adaptive secondary mirror of the telescope.

1.1 Measurements and atmospheric parameters

Metric data of the atmosphere is gathered by the three laser WFS*, the one TT-WFS, and an external DIMM-MASS[3,4] instrument. These five sensors yield a wealth of information about the atmosphere. The entire atmosphere, however, can only be measured by the TT-WFS and the DIMM-MASS instrument. From the TT-WFS the TT-mode of the atmosphere in the direction of the TT-star is measured and the DIMM-MASS instrument measures the seeing as well as a coarse atmospheric profile. The three LGS-WFS measure the lower atmosphere only. Each of them can measure the high order (HO-)wavefront error, i.e., Zernike 4 and higher, produced by the lower atmosphere in the direction of each LGS. Combining every two WFS-signals one can extract the C_N^2 profile of the lower atmosphere by a SLODAR[5] measurement and, via a (temporal) Periodogramm of the (spatial) power spectrum of the wavefront,[6] the wind profile with height.

Adaptive Optics Systems II, edited by Brent L. Ellerbroek, Michael Hart, Norbert Hubin, Peter L. Wizinowich,
Proc. of SPIE Vol. 7736, 77364R · © 2010 SPIE · CCC code: 0277-786X/10/$18 · doi: 10.1117/12.856982

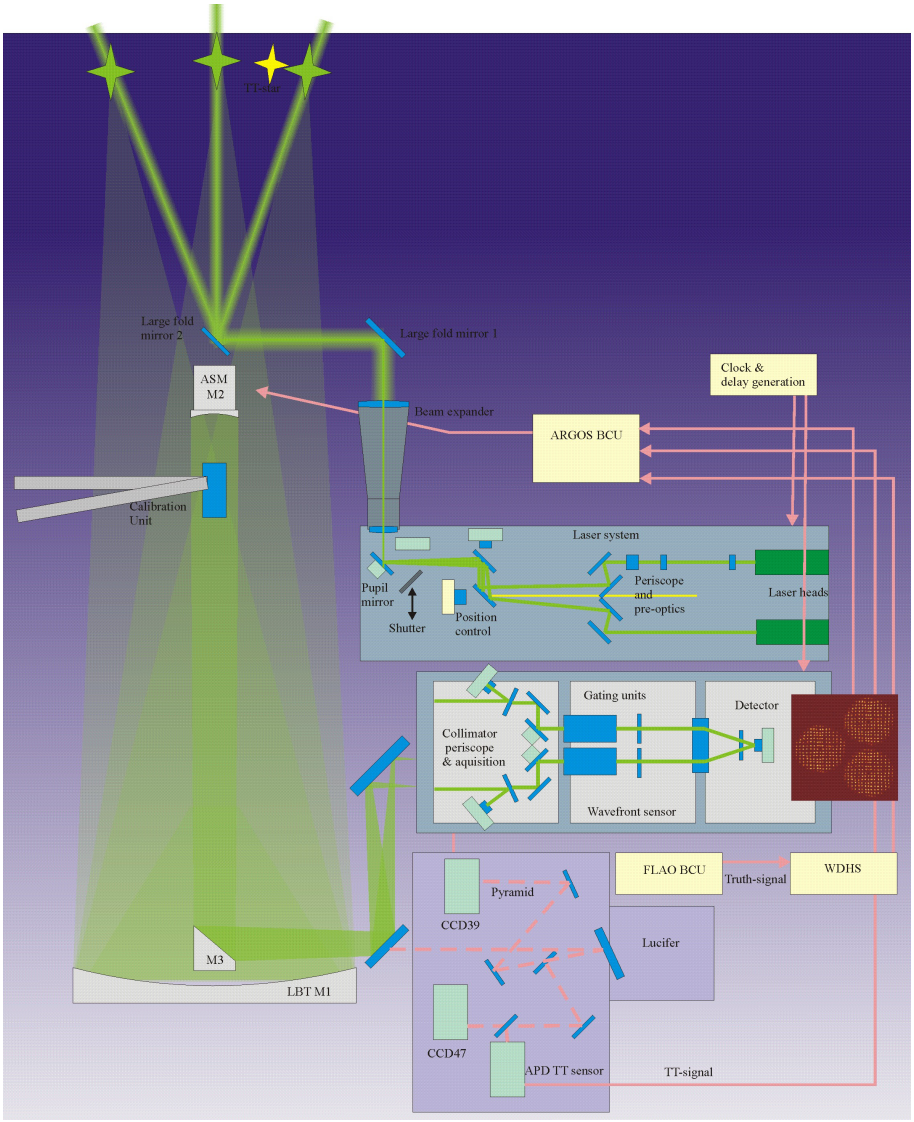

Figure 1. Sketch of the ARGOS system (courtesy of Sebastian Rabien)

Table 1. Measured and calculated parameters of the atmosphere

	Measurement	Parameter	Method
single laser WFS*	slopes	HO-modes	AO reconstruction
two laser WFS*	slope spatial correlations	C_N^2 profile	SLODAR
two laser WFS*	slope spatio-temporal correlations	wind profile	SLODAR, Fourier components
TT WFS	slopes	TT-modes	AO reconstruction
DIMM-Mass	Differential Image Motion	seeing, C_N^2 profile	DIMM-MASS

Table 1 outlines the different measurements and the parameters which can be extracted from the measurement and the method how this is done. From this wealth of information only the pure spatial measurements will be used in the following. Never the less the wind profile is mentioned for completeness. It could be used for

Further author information: (Send correspondence to D.Peter)
D.Peter: E-mail: peterd@mpia.de, Telephone: 0049 6221 528351
*Note that the laser only probes the atmosphere up to 12 km height

wavefront prediction. This prediction, however, is not subject of this paper.
The remainder of this paper is structured as follows: In Section 2 I will lay out the standard approach of PSF reconstruction. Section 3 outlines the additional difficulties the PSF reconstruction for ARGOS is facing. The entire reconstruction scheme is then presented in Section 4. The measure to test the accuracy of this reconstruction is defined in the following Section 5. The set-up of the simulations is described in section 6. The results are then presented in Section 7. Finally the paper is concluded with section 8.

2. POINT SPREAD FUNCTION RECONSTRUCTION

Post processing of astronomical data is an important task to optimize and characterize the image quality. In this context point spread function (PSF)-reconstruction is the tool required to enhance the scientific return by providing a quantitative measure of the resolution of the image produced by an AO-system. This means that knowledge of the spatial variation of the PSF over the entire field of view is desired. With this knowledge one can then separate the intrinsic source spatial properties from the spatially variable instrumental PSF by either: (i) convolving a model of the source with the PSF and comparing the result to the data, or (ii) deconvolving the image with the PSF and removing, at least partially, the speckles which are present in any image produced with an AO system. In either case, the structure of the targets on the image is revealed more clearly. One classical example where this method is used are double stars or multiple systems where the companion(s) sit on the PSF of the primary, maybe even closer than the diffraction limit of the telescope. As a result, they cannot be seen directly on the image, but after a PSF deconvolution the multiple nature of the target is revealed.

Two basic ingredients are needed for the reconstruction:

1. A reference PSF at one position of the image. This reference can be a bright star close to the target or a reconstructed PSF at one position of the image
2. A method to transfer the PSF from the reference to the positions of the other targets on the image. Classically this is done by the so called anisoplanatic transfer function (ATF)[7]

It is important to realise that I cannot just copy the approaches cited above because ARGOS has several features which are not covered within the studies found in the literature. These are:

1. Three laser guide stars and one TT-star are used
2. The position of the TT-star and the laser guide stars differ
3. Lasers which show cone effect
4. Mostly the lower layers of the atmosphere are probed only

2.1 Classical PSF-reconstruction

As the classical scheme of on-axis PSF reconstruction is an integral part of the extended scheme used for ARGOS PSF reconstruction I shortly summarize this approach.
The reconstruction of the on-axis PSF has been described by Veran et al.[8] and the algorithm has been improved later by Gendron et al.[9] This improvement has, however, not changed the basic principle. So in the following I will just sketch the Veran paper. A simplified version of the reconstruction scheme can be found in Figure 2.
The basic approach is to write the OTF of the system as a product of the OTF constructed from the modes measured by the WFS, $B_{\parallel}$, the OTF of the wave front orthogonal to the measured one, $B^{\perp}$, and the OTF of the (quasi-)static non-common-path aberrations, B_s.
B_s can be measured with a calibration source, so in the following I will only address the measurement of $B_{\parallel}$ and $B^{\perp}$.
In a first step one derives the noise transfer function Hn(g,f) from the modal gains g (Gendron & Lena[10]). Together with the noise on the gradients one can deduce the noise on the wave front. This is then expressed in terms of a noise covariance matrix, C_{nn}.

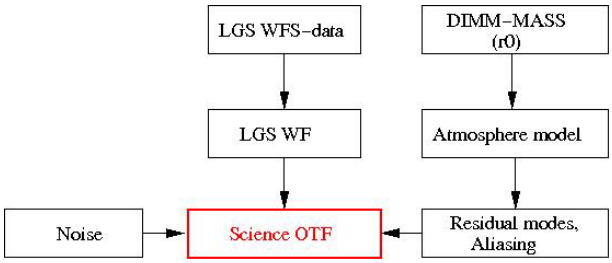

Figure 2. Basic scheme of the classical PSF reconsruction

One then uses the measurements of the atmospheric turbulence (C_N^2) to model the atmosphere either analytically or numerically. This model then provides the statistics of the HO modes not measured by the WFS. Together with the reconstruction matrix the model yields the aliasing measured on the WFS. The only missing parameter is the scale factor $(D/r_0)^{5/3}$. This factor can be derived iteratively using the noise on the wave front, the aliasing, and the mirror shape. This aliasing is then expressed as Covariance matrix C_{rr}. Also the model yields the covariance matrix of the not-corrected wave front as input for $B_\perp$. The last contribution comes from the measured wave front error σ_w^2 which is taken into account in the covariance matrix C_{ww}.
From the covariances C_{ww}, C_{nn} and C_{rr} one can compute the estimate of the true wave front covariance C_{tt} as $C_{tt} = C_{ww} - C_{nn} + C_{rr}$. From this one can compute $B_\parallel$. Putting $B_\parallel$, $B^\perp$, and B_s together one gets the science OTF and via FFT the on-axis PSF.

2.2 Transfer of the PSF in the desired angle on sky

One approach to derive a good estimate of the PSF in any angle on sky away from the guide star is to use the ATF.[7] The ATF is derived from atmospheric statistics (i.e. C_N^2-profile and Kolmogorov/van Karman spectrum). As the name already states it takes the anisoplanatism over the FOV into account. The final PSF is then the Fourier transform of the product of the on-axis (guide star) OTF with the ATF.
The ATF can be derived from inter-aperture correlations of the atmospheric modes, e.g., Zernike modes (see[11]). Another possibility to derive the PSF at any position in the field is to directly estimate the wave fronts in the desired field position from the WFS data.[12] This will be called 'projection' in the following. This projection can be applied directly to the covariance matrices, e.g. $B_\parallel$, and does not lead to a significant increase in computational needs. I will follow this approach in this paper.

3. DIFFERENCES TO THE STANDARD SOLUTIONS

As already mentioned in the introduction, in our case there are some additional challenges to solve. In the following I will do this one by one and in the end show the resulting scheme of the PSF reconstruction.

3.1 Finite Height of Laser

If one wants to evaluate the wave front from WFS data as stated in section 2.1 one has to split the wave front into the part which is measured by the WFS, i.e., the modes which have been calibrated, and the part orthogonal to it. In the case of the laser, however, not the full disturbance by the atmosphere is measured for any mode, but only for the atmosphere below the laser. The way to account for the turbulence not measured in the WFS is similar as in the case of a natural guide star. The only difficulty is to get the missing information on the atmosphere above the laser.
For the atmospheric modes which are not measured the important value I need to know is r_0. To get the right contribution of the higher atmospheric layers which are not measured, one can measure the C_N^2 profile of the entire atmosphere with the DIMM-MASS. The lower atmosphere will be measured with the three laser WFS using a SLODAR technique. With this scheme the Fried-parameter r_0^{tot} of the entire atmosphere and the Fried parameter of the lower atmosphere r_0^{low} can be measured. For the upper atmosphere r_0^{up} can be calculated via:

$$r_0^{up} = ((r_0^{tot})^{-5/3} - (r_0^{low})^{-5/3})^{-3/5} \quad (1)$$

With an atmospheric model I then estimate the contribution to $B_\perp$ of the high atmosphere in the same way as it is done for the not measured modes in the classical approach.

3.2 Different Sources of TT and HO signals

Using different sources of TT-modes and HO-modes is an additional item which makes the scheme more complex than the standard one. However, due to a correlation between Zernike modes for different directions on sky one can estimate the signals in the science direction given measurements in any direction on sky[†](see e.g. Whiteley et al.[12]). There are several possibilities for which signal to project in which directions in order to finally end up with the science signal. The approach yielding the least error due to the projection seems to be to project the three lasers into science direction and do the same for the TT-measurements. Thus the HO modes of the wave front is measured up to finite height and the TT modes of the wave front to infinite height.
Note that there exists also a scheme to improve the TT-estimate over the field by incorporating the HO-laser measurements.[13]

3.3 Three HO-Wavefront References

As already stated in the last section the target wave front will be calculated from the wave fronts of the three lasers and the one TT-star. This projection can be done using all three lasers simultaneously. The scheme is the same as for the support of the TT-estimation by the laser measurements[13] (see also Section 3.2).

3.4 Cone Effect

The cone effect is accounted for in the projection scheme for the wave fronts.[12]

4. THE FULL RECONSTRUCTION SCHEME

After the discussion of the single points which differ from the classical PSF reconstruction I will shortly outline the PSF reconstruction which will be used for ARGOS.
The full scheme of PSF reconstruction is shown in Figure 3. From the LGS WFS data and the TT WFS data the wavefront is reconstructed in the direction of the lasers and the TT star respectively. This is done from the measured mode vectors. In combination with the mirror shape and the C_N^2 profile measurements form SLODAR and DIMM the wave fronts are then projected via an optimized weighted minimum mmean square error (MMSE) projector into the desired direction (here on-axis).
The SLODAR itself makes use of the three LGS wavefront measurements in combination with the mirror shape.

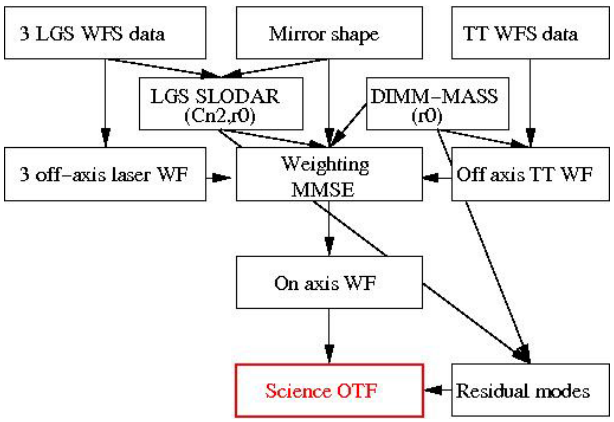

Figure 3. The PSF-reconstruction scheme for ARGOS

After projection into the desired direction on sky the PSF is reconstructed using the classical scheme with the wave front constructed above as input.

[†]Within a sufficiently small angle e.g. a few arcmin

5. MEASURE OF RECONSTRUCTION ACCURACY

To quantify the quality of the reconstruction, a measure is needed which can express the improvement due to PSF reconstruction. For imaging, for example, the final measure will be the photometric or astrometric accuracy on the science image. However, for a more technical description which is closer to the functionality of the reconstruction scheme the wave front root mean square (RMS) would be used. This is a more direct measure as the effect of the reconstruction on the science image also depends on the deconvolution algorithm (Jolissaint et al.[16]). The wave front RMS is also a good starting point for further investigations.
Still as it is very intuitive, to estimate the quality of the PSF reconstruction I will compare the radial profiles of the PSF on the science image and of the reconstructed PSF.

6. SIMULATIONS

To test the algorithm proposed for the PSF reconstruction, end to end simulations within CAOS[14] were performed. The following sub-sections describe the set up of the simulations and the results. These simulations are improved compared to the simulations presented in Peter & Gässler[15] as the simulations presented here now include the full ARGOS system with three lasers at finite height and a multi layered atmosphere.

6.1 Simulation Set-up and Parameters

Table 2. Basic simulation parameters

Laser positions at 2 arcmin	(0,120,240)
number of atmospheric screens	5
TT star at	2.5 arcmin (150)
Total Integration time	0.2s
Delay time of system	0
r_0@500 nm	0.1m (seeing 1)
Heights of layers	0m, 1000m, 3000m, 5000m, 10000m
Wind speed	3m/s, 5m/s, 8m/s, 10m/s, 12m/s
Frame rate	1 kHz

The simulations of the ARGOS system were set up as follows. As there is no real testing of the algorithm in any wave front not seen by the system, the entire atmosphere was placed below the lasers. Three different atmospheric profiles were used.

The main parameters of the simulation are summarized in Table 2. C_N^2 profiles for the three set-ups are presented in Table 3 and shown in Figure 4.

Table 3. The three different C_N^2 profiles

	C_N^2
1	0.65, 0.15, 0.1, 0.05, 0.05
2	0.1, 0.2, 0.4, 0.2, 0.1
3	0.05, 0.05, 0.1, 0.15, 0.65

7. RESULTS

In this section the results of the simulations for the three different atmospheric profiles are shown. In the beginning of every subsection the true image and the reconstructed one are presented. As the integration times of the simulations are so short, the result is a speckle image. To compare the simulated PSF with the reconstruction a radial profile of the image is calculated. This is done by averaging the values on a circle around the brightest spot on the image. The PSF is then normalized to 1 at the maximum. The result and the difference between the true profile and the reconstructed one are shown for typical examples.

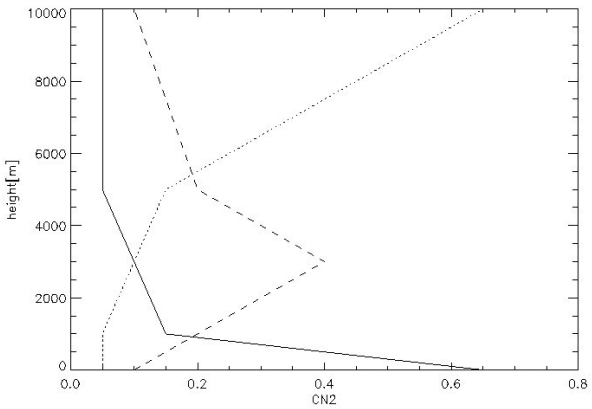

Figure 4. C_N^2 profiles: The solid line is the profile of model 1 (the standard Mount Graham atmosphere), the dashed one the profile of model 2, and the dotted one the profile of model 3.

7.1 Atmosphere Model 1

Figure 5 shows the simulated image and reconstructed image of the on-axis star from the simulation with the C_N^2 profile decreasing with height. The radial profiles in Figure 6 are very similar. The difference between the two is 1% of the maximum of the PSF in the centre and less towards the wings. So the PSF reconstruction is very good

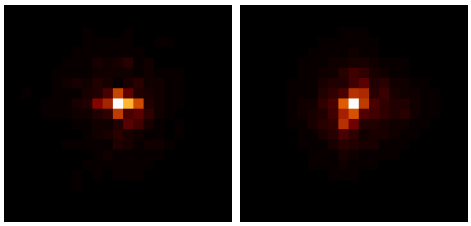

Figure 5. Image in K-band: Left: The image on the science camera, right: The image reconstructed from wavefront sensor data.

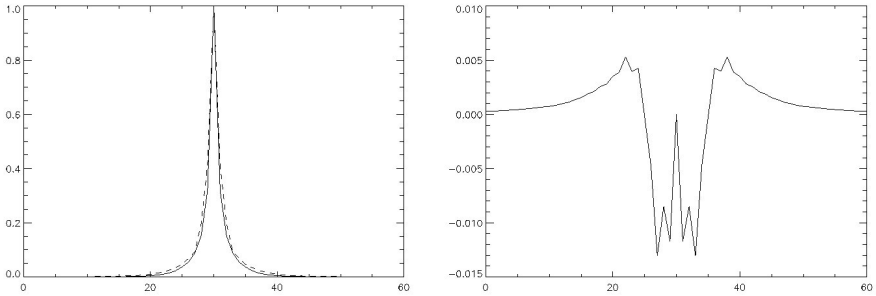

Figure 6. Left: The radial profiles of the two PSFs vs pixel number. The solid line shows the PSf of the science image, the dashed line the reconstructed PSF. Right: The difference between the two PSFs vs pixel number, the maximum difference is below 0.01 of the peak height.

.

7.2 Atmosphere Model 2

Figure 7 shows the image and reconstructed image of the on-axis star from the simulation with the C_N^2 profile with the maximum at 3 km. The radial profiles in Figure 8 are still similar. The difference between the two is however larger than 13% of the maximum of the PSF at the half-maximum point, and still significant close to the centre. A change in the normalization of the PSF from the normalization of the peak height to a normalization of the area under the PSF reduces the maximum difference between the two PSFs to below 8%. So even for this unconvenient atmospheric profile the reconstruction of the PSF is acceptable.

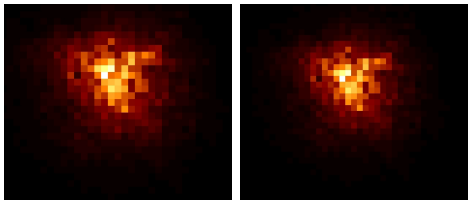

Figure 7. Image in K-band: Left: The image on the science camera, right: The image reconstructed from wavefront sensor data.

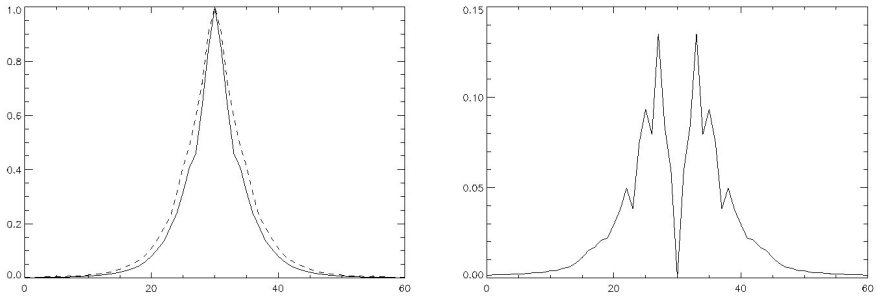

Figure 8. Left: The radial profiles of the two PSFs vs pixel number. The solid line shows the PSf of the science image, the dashed line the reconstructed PSF. Right: The difference between the two PSFs vs pixel number, the maximum difference is about 0.13 of the peak height.

7.3 Atmosphere Model 3

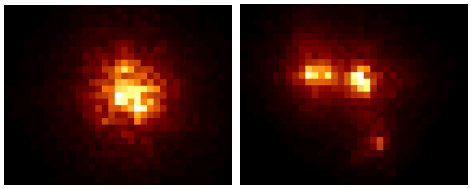

Figure 9. Image in K-band: Left: The image on the science camera, right: The image reconstructed from wavefront sensor data.

Figure 9 shows the image and reconstructed image of the on-axis star from the simulation with a C_N^2 rising with height. The reconstructed PSF is too narrow (Figure 10). As can be seen in Figure 8 this reconstructed PSF has two peaks. So a longer integration, which should have the peak centred, will probably have a larger size and come closer to the real PSF. This, however, needs to be verified in more extended simulations.

With the shift of the main turbulence to greater heights the performance of the system as well as the accuracy of the reconstruction are reduced more and more. This is obviously the case as the footprint of the laser beam decreases with height.

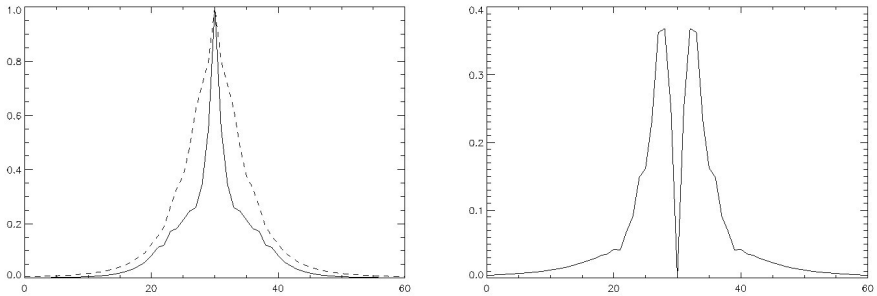

Figure 10. Left: The radial profiles of the two PSFs vs pixel number. The solid line shows the PSf of the science image, the dashed line the reconstructed PSF. Right: The difference between the two PSFs vs pixel number, the maximum difference is almost a third of the peak height.

8. CONCLUSIONS

I presented the scheme for PSF reconstruction for the GLAO system ARGOS. This scheme faces some additional difficulties compared with classical PSF reconstruction schemes for AO systems with a single natural guide star. These additional difficulties include: multiple sources, the use of laser guide stars, and the use of a single TT-star. After the discussion of the solutions for these features the scheme was tested in end-to-end simulations for three atmospheric models: one with most of the turbulence in the ground layer, one with a peak in turbulence strength in mid-height, and one with most of the turbulence shortly below the laser height. The agreement between the reconstructed on-axis PSF and the real on-axis PSF was very good in the first case aceptable for case two but in the case of strong high layer turbulence the difference between image and reconstructed image is significant. This difference, however, might be less in the case of longer integration times. This will be investigated in the future.

ACKNOWLEDGMENTS

The author wants to thank the ARGOS team especially W.Gässler for helpful discussions. ARGOS is partly funded through the European Framework Program 7 within OPTICON (grant agreement no 226604).

REFERENCES

[1] Rabien, S. et al., "ARGOS the laser guide star system for LBT", 7736-13 (this conference)
[2] Mandel, H. et al., "LUCIFER status report: summer 2008", Proc.SPIE, 7014, 124 (2008)
[3] Tokovinin, A. A., "From Differential Image Motion to Seeing", PASP, 114, 1156 (2002)
[4] Tokovinin, A. A. et al., "Statistics of turbulence profile at Cerro Tololo", MNRAS, 340, 52 (2003)
[5] Wilson, R. W., "SLODAR: measuring optical turbulence altitude with a Shack-Hartmann wavefront sensor", MNRAS, 337, 103 (2002)
[6] Poyneer, L. et al., "Experimental verification of the frozen flow atmospheric turbulence assumption with use of astronomical adaptive optics telemetry", JOSAA, 26, 833 (2009)
[7] Britton, M. C., "Analysis of crowded field adaptive optics image data", Proc.SPIE, 6272, 97 (2006)
[8] Veran, J.-P. et al., "Estimation of the adaptive optics long-exposure point-spread function using control loop data", JOSAA, 14, 3057 (1997)
[9] Gendron, E. et al., "New algorithms for adaptive optics point-spread function reconstruction", A&A, 457, 359 (2006)
[10] Gendron, E. & Lena, P., "Astronomical adaptive optics. 1: Modal control optimization", A&A,291, 337 (1994)
[11] Steinbring, E. et al., "Characterizing the Adaptive Optics Off-Axis Point-Spread Function. II. Methods for Use in Laser Guide Star Observations", PASP, 117, 847 (2005)
[12] Whiteley, M. R., "Optimal modal wave-front compensation for anisoplanatism in adaptive optics", JOSAA, 15, 2097 (1998)
[13] Peter, D., "An optimized controller for ARGOS: using multiple wavefront sensor signals for homogeneous correction over the field", 7736-40 (this conference)
[14] , Cabillet, M. et al., "Modelling astronomical adaptive optics: I. The software package CAOS", MNRAS, 356 (4), 1263 (2005)
[15] Peter, D. & Gässler, W., "Reconstruction of the point spread function for the ground layer adaptive optics system ARGOS", aoel.conf, 09004 (2010)
[16] Jolissant, L. et al., "Exploring the impact of PSF reconstruction errors on the reduction of astronomical adaptive optics based data", Proc.SPIE, 7015, 159 (2008)